Advances in Bioscience and Biotechnology, 2014, 5, 603-616
Published Online June 2014 in SciRes. http://www.scirp.org/journal/abb
http://dx.doi.org/10.4236/abb.2014.57071

Spontaneous and Bleomycin-Induced γH2AX Signals in CHO9 Metaphase Chromosomes

María Vittoria Di Tomaso[1], Silvia Basso[1], Laura Lafon-Hughes[1], Gustavo Saona[2], Beatriz López-Carro[1], Ana Laura Reyes-Ábalos[1], Pablo Liddle[1]

[1]Genetics Department, Instituto de Investigaciones Biológicas Clemente Estable, Montevideo, Uruguay
[2]Environmental Quality Evaluation and Control Service, Municipality of Montevideo, Montevideo, Uruguay
Email: marvi@iibce.edu.uy, silbasso@gmail.com, laulaf@iibce.edu.uy, gustavo.saona@gmail.com, bealc57@gmail.com, reyesabalos@gmail.com, pliddle@iibce.edu.uy

Received 26 March 2014; revised 22 May 2014; accepted 4 June 2014

Abstract

In eukaryotes, a cascade of events named DNA damage response (DDR) has evolved to handle DNA lesions. DDR engages the recruitment of signaling, checkpoint control, repair and chromatin remodeling protein complexes, allowing cell cycle delay, DNA repair or induction of apoptosis. An early DDR event involves the phosphorylation of the histone variant H2AX on serine 139 (H2AX^{139} phosphorylation) originating the so-called γH2AX. DDR-related H2AX^{139} phosphorylation have been extensively studied in interphase nuclei. More recently, γH2AX signals on mitotic chromosomes of asynchronously growing cell cultures were observed. We performed a quantitative analysis of γH2AX signals on γH2AX immunolabeled cytocentrifuged metaphase spreads, analyzing the γH2AX signal distributions of CHO9 chromosomes harboring homologous regions both in control and bleomycin (BLM)-treated cultures. We detected γH2AX signals in CHO9 chromosomes of controls which significantly increase after BLM-exposure. γH2AX signals were uniformly distributed in chromosomes of controls. However, the γH2AX signal distribution in BLM exposed cells was significantly different between chromosomes and among chromosome regions, with few signals near the centromeres and a tendency to increase towards the telomeres. Interestingly, both basal and BLM-induced γH2AX signal distribution were statistically equal between CHO9 homologous chromosome regions. Our results suggest that BLM exerts an effect on H2AX^{139} phosphorylation, prevailing towards acetylated and gene-rich distal chromosome segments. The comparable H2AX^{139} phosphorylation of homologous regions puts forward its dependence on chromatin structure or function and its independence of the position in the karyotype.

Keywords

H2AX Phosphorylation on Serine 139, γH2AX Signals, Metaphase Chromosomes, Homologous Chromosome Regions, CHO9 Chinese Hamster Cell Line

How to cite this paper: Tomaso, M.V.D., *et al*. (2014) Spontaneous and Bleomycin-Induced γH2AX Signals in CHO9 Metaphase Chromosomes. *Advances in Bioscience and Biotechnology*, **5**, 603-616. http://dx.doi.org/10.4236/abb.2014.57071

1. Introduction

DNA double-strand breaks (DSB) involve special challenges for the cells. DNA broken ends may rejoin with unexpected partners, producing chromosomal rearrangements. Besides, persisting DSB may lead to chromosome fragments loss during anaphase originating micronuclei. Unrepaired or mis-repaired DSB could lead to genomic or chromosomal instability, senescence, malignant transformation or cell death [1] [2]. In eukaryotes, a hierarchical and timely regulated cascade of events called DNA damage response (DDR) has evolved which includes the recruitment of signaling, checkpoint control, DNA repair and chromatin remodeling protein complexes. DDR allows cell cycle delay, DNA repair or induce cell dead by recruiting proteins of the apoptotic cascade [3]. An early DDR event engages the phosphorylation of the histone variant H2AX involving the oxygen in the γ-position of serine 139 in the C-terminal consensus serine-glutamine (SQ) motif ($H2AX^{139}$ phosphorylation) giving rise to the named γH2AX [4].

1.1. $H2AX^{139}$ Phosphorylation Related to DNA Damage Response

In response to DSB, Ataxia Telangiectasia Mutated (ATM) and other phosphoinositide-3-Kinase-related protein Kinases (PIKK) family, such as DNA-PK, phosphorylate $H2AX^{139}$ [4]. γH2AX acts as a recruiting site for the mediator of DNA damage checkpoint protein 1 (MDC1), a DDR-adaptor and signaling amplifier protein complex which in turn promotes the recruitment of MRN (*via* NBS1) and ATM, to again phosphorylate H2AX and MDC1. As a result, MDC1 creates a positive feedback loop for expanding H2AX phosphorylation bi-directionally up to 2 Mbp away [5], amplifying DNA damage signaling [6]. The $H2AX^{139}$ phosphorylation recruits checkpoint and repair proteins at DSB sites but also ubiquitin ligases (RNF8/UBC13 and RNF168/UBC13), chromatin remodeling complexes (*i.e.* 53BP1), histone acetyltransferases and cohesins that may prevent the dissociation of broken ends at DSB sites [7] [8].

Employing anti-γH2AX immunolabelling, chromatin regions harboring phosphorylated $H2AX^{139}$ can be detected in interphase nuclei as individual foci. γH2AX foci increase from 1 - 2 min up to 30 min after ionizing radiation, followed by a slow decline [5]. Foci are completely formed 10 min post-exposure and contain DSB repair factors indicating active DNA repair [9]. The bulk of foci disappear at 8 h post-irradiation, indicating DSB restoring [5]. The disappearance of damage induced-γH2AX foci could result either from γH2AX removal through histone exchange [10] or direct serine 139 dephosphorylation by protein phosphatases (including PP2A, PP4 and WIP1) [11] [12].

Interestingly, a number of γH2AX foci can be detected 48 h to 7 days after >1 Gy irradiation being attributed to incomplete repair of complex DSB, persistent chromatin alterations or apoptosis [13] [14]. Co-immunolabelling of γH2AX and DDR proteins has revealed that γH2AX foci temporarily change in composition due to recruitment or dissociation of proteins throughout the cell cycle. For instance, NBS1, MRE11 and 53BP1 dissociate from γH2AX foci at the G2/M transition to re-associate at early G1, whilst MDC1 remains throughout the cell cycle [15] [16].

Checkpoint pathways activated during the G1/S and G2/M cell cycle transitions prevent progression of cells bearing DNA damage to mitosis [17]. In cases of checkpoint failure, the antephase checkpoint, operating subsequently (between late G2 and mid prophase), can delay mitosis or reverse mitotic progression as well [18] [19]. Once these cell cycle checkpoints are passed, mammalian cells go through mitosis, even in the presence of DNA damage. A still poorly understood γH2AX immunostaining has been observed in mitotic chromosomes, probably related to these checkpoint pathways [16] [20]-[22], serving to facilitate DDR activation and accelerate DNA damage repair in the novel cell generation [22] [23].

1.2. $H2AX^{139}$ Phosphorylation Associated to Apoptotic Cascades

Apoptotic programmed cell death represents a multistep pathway involved in cell death during development, senescence or DNA and cellular stresses. γH2AX can be required for DNA fragmentation during apoptosis, being phosphorylated concomitantly with the initial formation of high molecular weight DNA fragments, although before internucleosomal DNA fragment production [24] [25]. H2AX may function in the crosstalk between cell survival and cell death in response to DNA damage depending on the balance between serine 139 phosphorylation and the constitutively tyrosine 142 phosphorylation by WSTF kinase. During DDR, dephosphorylation of -tyrosine 142 (by EYA1-3) is necessary for MDC1 binding. If tyrosine 142 dephosphorylation is not accomplished, the cellular response shifts to apoptosis with recruitment of pro-apoptotic factors [26].

In the case that the G1/S, G2/M or antephase checkpoint systems fail, cells can activate the death pathways during the mitotic process or also after mitotic exit [17] [27]. Since the same result was obtained when BLM-treated cells were exposed to the G2/M checkpoint inhibitor UCN-01 (a CHK1 inhibitor) post-mitotic death would not be the consequence of G2/M checkpoint failure [27]. This result suggests that persisting DNA damage during mitosis can enhance a delayed post-mitotic cell death program.

Moreover, stimuli apart from DNA damage can trigger the extrinsic apoptotic pathway with $H2AX^{139}$ phosphorylation. For instance, the tumor necrosis factor (TNF) superfamily originating the death-inducing signaling complex (DISC) at the cell surface [28] and the TNF-related apoptosis-inducing ligand TRAIL (a member of the TNF/death receptor superfamily) can induce the apoptotic pathway. Also, it was reported that TRAIL can also produce DDR with ATM, DNA-PK and $H2AX^{139}$ phosphorylation after 1 h of TRAIL exposure, without induction of DNA damage [29].

1.3. Scheduled or Cell Cycle Related $H2AX^{139}$ Phosphorylation

$H2AX^{139}$ is phosphorylated also in undamaged cells. A foci population reminiscent of large IR-induced foci that co-localized with many DSB repair proteins and a main population of γH2AX small foci that did not associate with repair proteins were documented in untreated asynchronic cultures of mammalian cells [21]. Large γH2AX foci may represent spontaneous DSB, while small foci are DSB-independent. Signal intensity of large and small foci increased through cell progression from G1 to S and G2 phases, reaching the highest intensity during mitosis, especially during metaphase [21].

Scheduled $H2AX^{139}$ phosphorylation originates when temporary DSB generate in the V(D)J and class-switch recombination during immune system development and also at sites of DSB formation in meiosis [30]. Additionally, in somatic cells lacking telomerase, where shortened telomeres behave as DSB, $H2AX^{139}$ is phosphorylated as well [31]. A cell cycle linked $H2AX^{139}$ phosphorylation, particularly takes place when DNA polymerase or RNA polymerase II stall at spontaneous DNA base alterations (mismatches, modified bases, abasic sites) inducing SSB during replication or transcription processes, respectively. In addition, when the resealing of DNA topoisomerase I or II cleavable complexes are blocked by collision with DNA polymerase or RNA polymerase II, producing SSB or DSB, H2AX can be also phosphorylated at serine 139 [32].

A cell cycle related $H2AX^{139}$ phosphorylation, in the absence of induced DNA damage, occurring during mitotic chromatin structural changes, was recently proposed. The status of $H2AX^{139}$ phosphorylation, during premature chromosome condensation (PCC) process induced by calyculin A was investigated in both human leukemic (HL60) and pulmonary carcinoma (A549) cells [33]. Interestingly, untreated A549 cells showed phosphorylated $H2AX^{139}$ while non-exposed HL60 cells did not display γH2AX signals. The authors reported a sequential phosphorylation, first on serine 10 of histone H3 and then on serine 139 of H2AX. The disparity in H2AX phosphorylation observed in different cell types suggests that it may be not a common attribute of mitotic chromosomes or a mandatory feature of chromatin condensation during mitosis [33].

It has been reported that some metaphases from untreated asynchronously growing cell cultures exhibit γH2AX signals all along the chromosomes. However, the yield and distribution of γH2AX signals was not analyzed so the extension of this phenomenon remains unclear. On the other hand, it is well established that clastogenic agents such as X-rays and bleomycin (BLM) induces $H2AX^{139}$ phosphorylation during interphase.

In this work, we carried out a quantitative analysis of γH2AX signals on chromosomes of cytocentrifuged control and BLM-treated metaphase spreads in order to characterize and compare γH2AX signal distribution (per metaphases and chromosomes) in the absence (basal γH2AX signals) and presence of DNA damage (BLM-induced γH2AX signals). Chromosomes were divided in three regions (proximal, medial and distal to the centromere) to test a differential sensitivity to $H2AX^{139}$ phosphorylation along the chromosomes. Besides, under the hypothesis that chromatin structure influences $H2AX^{139}$ phosphorylation, we selected eight CHO9 chromosomes harboring homologous regions (located in normal or rearranged chromosomes) to test if homologous regions harbor similar γH2AX signal distributions. In the same sense, one of the chromatin structure signatures, the profiles of H4 hyperacetylation was compared to γH2AX signal profiles.

2. Methodology

2.1. Selection of CHO9 Chromosomes

The CHO9 cell line is a subclone of CHO (Chinese hamster ovary) cells [34]. It is characterized by 21 chromo-

somes, containing nine original chromosomes (1, 2, 5, 7, 9, 10, two 8 and one X) plus twelve elements (Z1-Z10, Z12 and Z13) [35] originated by rearrangements occurring during the cell line transformation. To analyze γH2AX signals we selected eight chromosomes (1, Z1, 2, Z2, Z3, Z4, 5, Z6) which can be paired according to the presence of five homologous regions as a result of rearrangements, as follows: 1-Z1, 1-Z6, 5-Z6, 2-Z2; Z3-Z4. **Figure 4** shows DAPI-stained images and idiograms of these chromosomes; identical color coded bars indicate the partners of each homologous region: 5-Z6 (orange), 1-Z6 (light blue), 1-Z1 (violet), 2-Z2 (green), and Z3-Z4 (red).

2.2. Cell Culture

CHO9 cells (from Natarajan AT, Leiden) were cultivated in 95 mm Petri dishes with Ham-F12 (PAA E15-890) culture medium supplemented with 10% fetal calf serum (PAA A15-151), 200 mM glutamine and antibiotics (100 U/mL penicillin and 125 mg/mL dihydrostreptomycin sulfate) (Sigma) at 37˚C in a 5% CO_2 incubator.

2.3. Treatment

Exponentially growing CHO9 cells were treated with 10 µg/mL of the radiomimetic agent bleomycin (BLM) at 37˚C and 5% CO_2, during 30 min. Next, the culture medium was removed and the monolayer washed with PBS. The medium was centrifuged for 5 min at 800 rpm to collect mitotic cells which were resuspended in complete medium and incorporated into the culture. Immediately, 0.16 µg/mL Colcemid (Ciba) was added for 60 min at 37˚C and 5% CO_2. Considering the recovery time of 90 min after BLM-treatment, the cells recovered at metaphase stage were in the G2 phase or in early stages of mitosis during BLM exposure.

2.4. Metaphase Spreads

After colcemid exposure, mitotic cells were recovered, centrifuged for 5 min at 1200 rpm, re-suspended in 75 mM KCl at 37˚C at a final cell concentration of 5×10^6 cells/mL. After 10 min, the cell suspension was cytocentrifuged onto slides at 2000 rpm during 10 min, using a Cellspin I cytocentrifuge (Tharmac GmbH) to obtain metaphase chromosome spreads.

2.5. γH2AX Immunolabeling

Chromosomal preparations were fixed (2% paraformaldehyde, 5 min), permeabilized (0.5% Triton X-100, 5 min) and blocked (2% BSA, 15 min). Subsequently, slides were incubated with mouse monoclonal anti-γH2AX (Abcam, 1:500 in 2% BSA) for 30 min. After washing in 2% BSA, the preparations were incubated with rabbit Alexa 488-conjugated anti-mouse antibodies (Molecular Probes, 1:250 in 2% BSA) for 30 min. Finally, nuclei were counterstained (10 min) with 1.5 µg/mL DAPI (Sigma-Aldrich) and mounted in Vectashield (Vector Laboratories).

2.6. Image Acquisition and Analysis

Metaphase spread images from controls (n = 40) and BLM-exposed (n = 40) cultures were captured using an Axioplan Mot II fluorescence microscope (Zeiss) with 100x Neofluar phase contrast objective (N.A. 1.30) and FITC/DAPI filters. A scanning digital monochromatic camera (Metasystems CV-M4 + CL) and ISIS program (Metasystems) were employed for image acquisition with a fixed exposure time.

Using the Adobe Photoshop CS program, chromosome images of captured metaphases were karyotyped based on relative size, centromere position and DAPI banding patterns, to identify chromosomes 1, 2, 5, Z1, Z2, Z3, Z4 and Z6. Images of each chromosome either from control (n = 40) or BLM-treated cells (n = 40) were arranged horizontally side by side to the corresponding 229 CHO9 G-band ideogram [36] and their sizes adjusted to fix the respective ideograms. Chromosomes pertaining to the same metaphase were ordered vertically. Parallel lines were drawn to indicate on the images of DAPI/γH2AX stained chromosomes the regions matching the G-band ideogram.

2.7. Data Processing and Statistical Analysis

Based on our experimental design, BLM-damaged post-replicating cells were recovered 90 min after treatment

as well as post-replicating control cells. Therefore, H2AX 139 phosphorylation signals on each chromatid were considered as independent events. The absence of γH2AX signal in a band was scored as 0, a signal in only one chromatid band as 1 and parallel signals in both chromatids as 2. The first scores of γH2AX signals were referred to the G-bands of chromosomes 1, 2, 5, Z1, Z2, Z3, Z4 and Z6. Then, each chromosome was divided into three segments related to the centromere: proximal, medial or distal (PMD) regions of equal lengths. A score of γH2AX signals was also assigned to each PMD region through the addition of individual band scores. To enable comparisons, the scores were standardized by division between the relative lengths and the number of bands of each PMD region. Analogously, standardized scores of γH2AX signal on whole 1, 2, 5, Z1, Z2, Z3, Z4 and Z6 chromosomes were obtained. Likewise, a standardized score of γH2AX signal was assigned to each homologous region harbored in the eight selected CHO9 chromosomes (1-Z1, 2-Z2, Z3-Z4, 5-Z6 and 1-Z6). In addition, a raw band score adjusted by relative band length was added, band by band, to obtain a γH2AX signal profile along each chromosome. γH2AX signal score distribution in metaphases from control and BLM-treated cells of each whole 1, 2, 5, Z1, Z2, Z3, Z4 and Z6 chromosome, PMD and homologous chromosome regions were graphically represented, indicating 25th percentile (p25), below which were 25% of γH2AX signals, 50th percentile (p50), the median of γH2AX signal distribution, and 75th percentile (p75) below which were 75% of γH2AX signals. Since the variables (γH2AX signal scores of bands, PMD regions and chromosomes) did not follow a normal distribution (Shapiro-Wilk test) or showed homogeneity (Levene test), a more demanding and robust significance level (α = 0.001) was chosen when BLM-treatment, chromosomes, PMD and homologous regions were compared with ANOVA and *post hoc* Tukey or t-test. The non-parametric sign-test for paired samples was also applied to contrast medians of γH2AX signal distribution between the chromosomes, PMD and homologous regions.

3. Results

3.1. Distribution of γH2AX Signals in CHO9 Metaphases

As illustrated in **Figure 1**, metaphases of both control and BLM-treated CHO9 cells showed γH2AX signals. The regions of γH2AX signals observed in metaphase chromosomes were generally large, involving several chromosome bands. Quantification of signals along 1, 2, 5, Z1, Z2, Z3, Z4 and Z6 chromosomes in control (n = 40) and BLM-treated cells (n = 40) revealed a high dispersion in γH2AX signal distribution, ranging from no signal to nearly whole chromosome immunostaining.

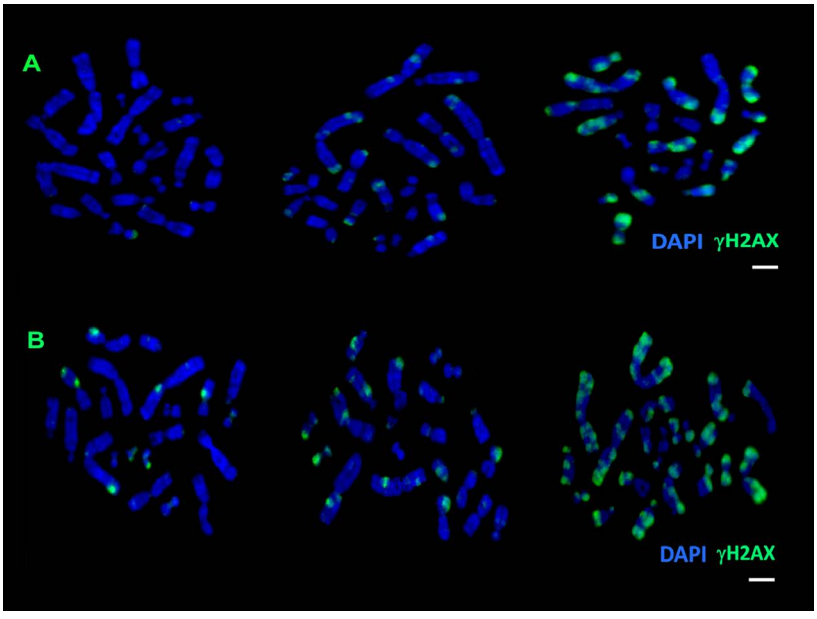

Figure 1. Examples of cytocentrifuged CHO9 metaphases of three control (A) and three BLM-exposed (B) cells showing γH2AX signals (green) on DAPI-counterstained chromosomes (merged images). Bars = 5 µm.

To characterize the chromosome γH2AX signal distribution, the percentiles p50 (median), p25 and p75 were calculated (**Table 1** and **Figure 2**). Although chromosomes of controls showed γH2AX signals, BLM-treatment significantly increased $H2AX^{139}$ phosphorylation. The percentiles p25, p50 and p75 of γH2AX signal distribution were higher in BLM-exposed than in control CHO9 cells (**Table 1** and **Figure 2**). Besides, the overall γH2AX signal distribution of control and BLM-exposed cells showed significant differences (ANOVA $p < 0.001$).

3.2. Distribution of γH2AX Signals along Different CHO9 Chromosomes

Figure 2 illustrates the distribution of γH2AX signals in the eight CHO9 selected chromosomes. The comparison of γH2AX signal distribution of each chromosome between controls and BLM-exposed cells showed significant differences (Tukey test, $p < 0.001$). The median of γH2AX signal distribution of each chromosome of controls was significantly lower than those of the BLM-exposed cells, highlighting that BLM-treatment increased $H2AX^{139}$ phosphorylation in all analyzed chromosomes. Within the control population, there were no differences between γH2AX signals of each chromosome (Tukey test, $p < 0.001$ and sign test, $p < 0.0001$). Nevertheless, in BLM-treated cells, non-parametric sign test revealed that the median of γH2AX signal in Z6 chromosome was significantly higher compared to other chromosomes ($p < 0.0001$). Furthermore, the medians of γH2AX signal distributions in CHO9 chromosomes showed a tendency to decrease as follows: Z6 > Z2 > 2 > 5 > 1 > Z4 > Z1 > Z3 (sign test, $p < 0.0001$).

3.3. Distribution of γH2AX Signals in PMD Chromosome Regions

Proximal, medial and distal (PMD) chromosome regions of equal lengths were assigned for each chromosome in order to analyze the influence of centromere or chromosome end proximities in the distribution of γH2AX signals. **Figure 3** shows the distribution (p25 to p75) and the median of γH2AX signals in control and BLM-treated cells. ANOVA ($p < 0.001$) and Tukey ($p < 0.001$) tests demonstrated that BLM-treatment significantly increased γH2AX signals in each region compared to controls. In the control population, the γH2AX signal distribution

Table 1. Sample sizes and parameters of γH2AX signal distributions in control and bleomycin-treated CHO9 cell populations.

	Metaphases (n)	Chromosomes (n)	PMD regions (n)	Bands (n)	γH2AX (p25)	γH2AX (p50)	γH2AX (p75)
Control	40	320	960	9160	0.00	0.59	4.71
BLM	40	320	960	9160	0.53	2.50	5.42
Total	80	640	1920	18320	0.53	1.67	5.00

BLM: bleomycin-treated CHO9 cells. n: pooled number of: metaphases; chromosomes 1, 2, 5, Z1, Z2, Z3, Z4 and Z6 (8 chromosomes × 40 metaphases); proximal, medial and distal (PMD) chromosome regions (3 PMD regions × 8 chromosomes × 40 metaphases); chromosome bands scored in controls or BLM-exposed CHO9 cells (229 bands/metaphase × 40 metaphases). p25: 25th percentile, p50: 50th percentile (median values), and p75: 75th percentile of γH2AX chromosome signal distributions.

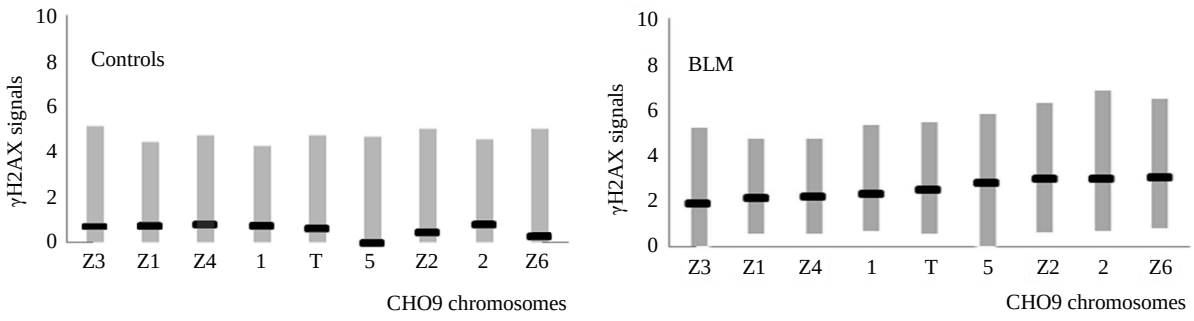

Figure 2. Bar-graph representing the distribution of γH2AX signals on CHO9 chromosomes of control and n = 40 BLM-treated (BLM) cells. Vertical grey bars represent the percentile range (p25 to p75) of γH2AX signal distribution on each chromosome. The median (p50) of the distribution is indicated by the horizontal black line on each bar. From left to right: Z3, Z1, Z4, 1, pooled chromosomes (T), 5, Z2, 2 and Z6.

was similar among PMD regions of the eight chromosomes (Tukey test, sign-test). In BLM-exposed cells, proximal regions revealed significant differences in γH2AX signal distribution (sign-test, $p < 0.0001$), exhibiting less $H2AX^{139}$ phosphorylation than medial or distal regions. Moreover, a tendency to higher $H2AX^{139}$ phosphorylation in the distal chromosome regions was observed (**Figure 3**).

3.4. γH2AX Signal Distribution between Homologous Regions of CHO9 Chromosomes

The homologous regions of the eight rearranged CHO9 chromosomes are shown in **Figure 4**. Distinct color bars illustrate the location and extension of the homologous chromosome regions. Partners of each homologous region are depicted with the same color bars.

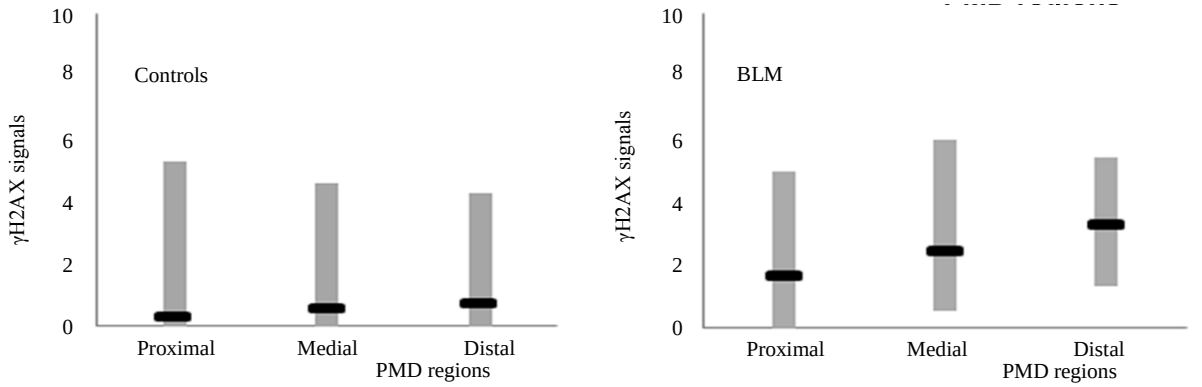

Figure 3. Bar-graph representing the distribution of γH2AX signals considering pooled proximal, medial and distal (PMD) regions of CHO9 chromosomes from control and BLM-treated (BLM) cells. Vertical grey bars represent the percentile range (p25 to p75) of γH2AX signal distribution on each PMD chromosome region. The median (p50) of the distribution is indicated by the horizontal black line on each bar. From left to right in both controls and BLM: pooled distal, medial and proximal chromosome regions.

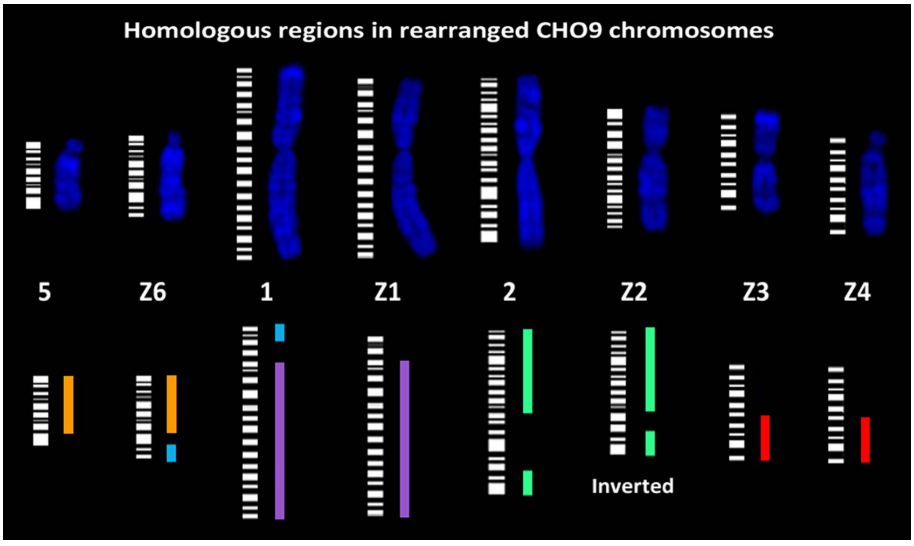

Figure 4. Homologous regions in CHO9 rearranged chromosomes. Images of DAPI-stained (blue) 1, 2, 5, Z1, Z2, Z3, Z4 and Z6 chromosomes aligned to the respective G-banding ideogram are depicted. Color bars at the right side of each ideogram indicate homologous regions between 5 and Z6 (orange), 1 and Z6 (light blue), 1 and Z1 (violet), 2 and Z2 (green), and between Z3 and Z4 (red), originated through chromosome rearrangements. Z1 and the acrocentric Z6 derived from a reciprocal translocation (1:5) involving distal regions of 1p and 5q. Chromosome Z2 arose from a 2q deletion. A pericentric inversion of chromosome 3 involving entirely 3p and the proximal portion of 3q generated acrocentric Z4. A translocation (3p; 4p) produced Z3 [35].

With the aim to test whether homologous regions behaved similarly or not with respect to γH2AX signal distribution, we contrasted them between the homologous regions in each pair of chromosomes (*i.e.* 1-Z1) and then, we compared these distributions between all five homologous regions, both in controls and BLM-exposed cells. The median and the p25 to p75 range of γH2AX signal distributions in homologous regions (1-Z, 1-Z6, 2-Z2, Z4-Z3 and 5-Z6) of control and BLM-treated cells are shown in **Figure 5**.

The overall γH2AX signals in homologous regions were significantly higher in BLM-treated than control cells (ANOVA, $p < 0.001$). Either in controls or BLM-exposed cells, the distribution of γH2AX signals between the homologous regions of each chromosome pair was similar (t-test, $p > 0.98$). However, γH2AX signals distribution showed significant differences between homologous regions located in distinct chromosome pairs (t-test, $p < 0.001$; sign-test, $p < 0.0001$). Homologous regions in 1-Z1 and Z3-Z4 displayed lower $H2AX^{139}$ phosphorylation than 5-Z6 and 1-Z6. Interestingly, chromosome 1, which harbors both 1-Z1 and 1-Z6 homologous regions (**Figure 4** and **Figure 5**), exhibited higher $H2AX^{139}$ phosphorylation on the latter (t-test, $p < 0.001$; sign-test, $p < 0.0001$).

3.5. Comparison between Chromosome γH2AX Signals and Hyperacetylated Regions

Figure 6(A) depicts γH2AX signal profiles of CHO9 chromosomes harboring homologous regions of both controls and BLM-exposed cells. **Figure 6(B)** compares chromosomal γH2AX signal profiles with the corresponding $H4^{+ac}$ pattern of BLM-treated cells. Both profiles are referred to G-bands ideograms. The patterns of $H4^{+ac}$ in CHO9 chromosomes were previously established in our laboratory [37], using an antibody that recognizes di-, tri- and tetra-acetylated lysine 12 of histone H4 (H4K12ac).

As can be observed in **Figure 6(B)**, similarities between γH2AX and $H4^{+ac}$ profiles were observed for each analyzed chromosome. Additionally, a tendency of both profiles to increase towards terminal chromosome regions mainly in BLM-exposed cells was detected.

4. Discussion

In the present work, a quantitative analysis of spontaneous or BLM-induced γH2AX signals on CHO9 metaphase chromosomes was addressed.

4.1. Spontaneous γH2AX Signals Were Observed in Control Metaphases

Since CHO9 control metaphases exhibited noticeable γH2AX signals (**Figure 1**) one may assume the presence of $H2AX^{139}$ phosphorylation independent of DNA damage. Cell cycle-dependent $H2AX^{139}$ phosphorylation in nocodazole synchronized human cells confirmed through γH2AX immunostaining and western blot analysis was reported [20]. γH2AX foci were observed in a small proportion of interphase nuclei but in nearly all mitotic chromosomes, reaching the maximum level at metaphase. However, γH2AX induction in mitotic chromosomes

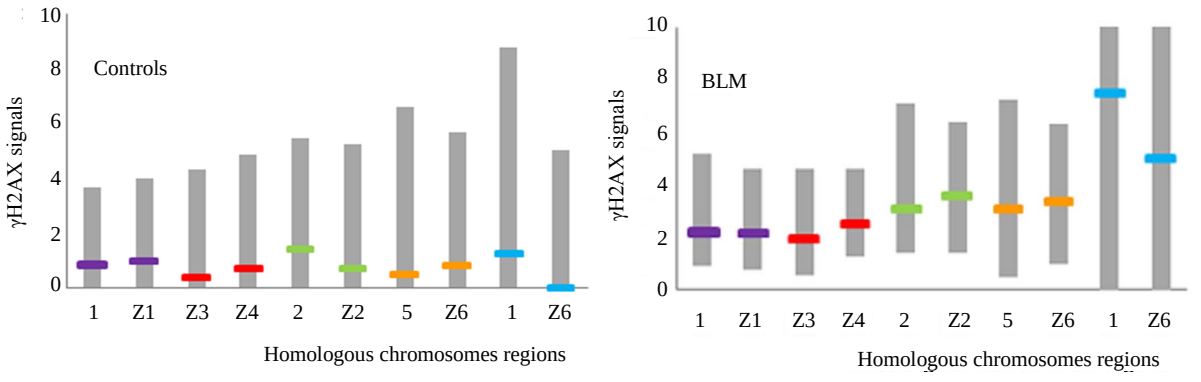

Figure 5. Bar-graph representing the distribution of γH2AX signals in homologous regions of CHO9 chromosomes. Vertical grey bars represent the percentile range (p25 to p75) of γH2AX signal distribution of each homologous chromosome region. The median (p50) of the distribution is indicated by the horizontal line on each bar. From left to right in both controls and BLM: 1 and Z1 (violet), Z3 and Z4 (red), 2 and Z2 (green), 5 and Z6 (orange) as well as 1 and Z6 (light blue) homologous regions.

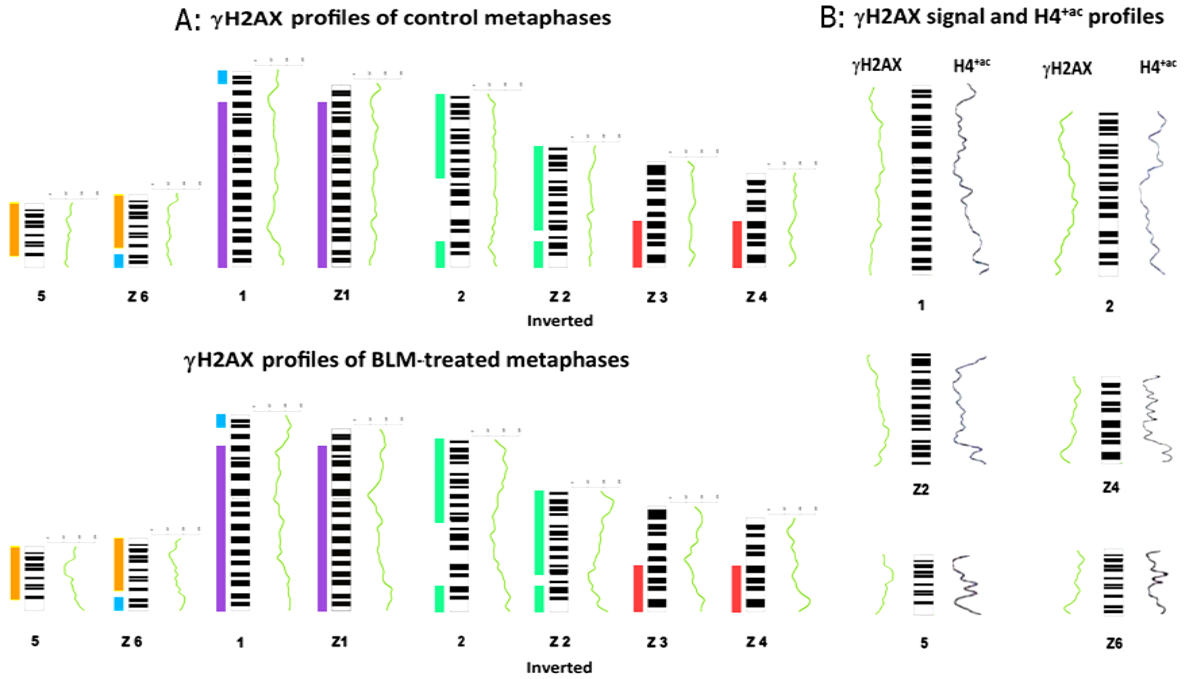

Figure 6. (A) γH2AX and $H4^{+ac}$ signal profiles of CHO9 chromosome harboring homologous regions of both controls and BLM-exposed cells. Homologous regions (bars) shared by chromosomes 5 and Z6 (orange), 1 and Z6 (light blue), 1 and Z1 (violet), 2 and Z2 (green), as well as between Z3 and Z4 (red) are shown at the left side of each ideogram. γH2AX signal profiles are illustrated at the right side of each ideogram. (B) γH2AX and $H4^{+ac}$ signal profiles are respectively depicted at the left and right sides of ideograms corresponding to chromosomes 1, 2, Z2, Z4, 5 and Z6. γH2AX signal profiles belong to BLM-treated cells. The chromosome patterns of $H4^{+ac}$ were previously established in our laboratory [37].

was not associated with CHK2 or p53 signaling protein phosphorylations, suggesting that in this context H2AX phosphorylation is independent of DNA damage response [20].

In this respect, the role of mitotic chromosome condensation on $H2AX^{139}$ phosphorylation should be considered. It was reported that mitotic γH2AX induction takes place in parallel with histone H3 phosphorylation at Ser 10 by Aurora kinase [38]. Since H3 phosphorylation at Ser 10 is considered a cytogenetic mark of chromatin condensation during mitosis [39], it was suggested that mitotic γH2AX could play a role in proper condensation of chromatin [20]. Furthermore, mitotic γH2AX could arise in response to the tensional stress generated during mitotic chromatin remodelling, turning DNA more sensitive to nucleases [40].

Besides, chromatin condensation along mitosis could explain the presence of large γH2AX signals observed in CHO9 metaphase chromosomes. Large γH2AX signals may arise by recruitment of single γH2AX focus during chromosome condensation. Since γH2AX signals enlarge on swollen metaphase chromosomes of HeLa and *Indian muntjac* cells, aggregation of individual γH2AX foci producing a large γH2AX signal may take place [16].

Furthermore, G2/M and antephase checkpoints are not only sensitive to DNA damage, but also to a variety of insults such as hypothermia, anoxia, osmotic shock or even to non-clastogenic drugs like colcemid or nocodazole [41] [42].

During the experimental procedures, CHO9 cells could be stressed by colcemid treatment, hypothermia or osmotic changes activating pathways involved in $H2AX^{139}$ phosphorylation. However, since γH2AX signals were previously detected on mitotic chromosomes of asynchronously growing cell cultures not exposed to colcemid [16] [20]-[23], this compound may not impact on $H2AX^{139}$ phosphorylation.

It must be taken into account that a proportion of CHO9 basal γH2AX signals could be related to persisting scheduled $H2AX^{139}$ phosphorylation due to temporary SSB or DSB induced during replication or transcription [30] [31] [43]. Besides, SSB or DSB produced by endogenous oxidative DNA damage along DNA replication could also contribute to γH2AX signaling. Additional experimental approaches are needed to deepen our understanding of $H2AX^{139}$ phosphorylation unrelated to the DNA damage response, especially γH2AX induced dur-

ing mitosis.

4.2. BLM-Exposure Increased γH2AX Signals on Metaphase Chromosomes

Although metaphase chromosomes of control cells showed γH2AX immunolabelling, BLM-treatment increased mitotic $H2AX^{139}$ phosphorylation (ANOVA, $p < 0.001$). Occurrence of γH2AX signals during mitosis after DNA damage induction has been previously reported [16] [20] [21] leading to the assumption that persisting γH2AX signals may serve to facilitate DDR in the novel cell generation [22] [23]. Thus, the observed γH2AX signal increase in CHO9 metaphases treated with BLM could correspond to a DDR related $H2AX^{139}$ phosphorylation persisting through mitosis.

Further, when chromosomes were exposed to γ-rays or treated with adriamycin during mitosis, strong γH2AX signals as well as elevated rates of segregation and cytokinesis failures were observed [44] [45]. This could mean that $H2AX^{139}$ phosphorylation not only occurs in interphase nuclei, but also could arise during mitosis.

4.3. Spontaneous and BLM-Induced γH2AX Signals Varied between Metaphases

High dispersion in the overall level of γH2AX signals between CHO9 metaphases was observed ranging from complete absence to nearly whole immunostained metaphases (**Figure 1**). Several factors competent for $H2AX^{139}$ phosphorylation could combine, inducing a particular level of γH2AX signal in a metaphase. For instance, extensive metaphase immunostaining could result from BLM-exposure plus a contribution of endogenous SSB and DSB, originated during DNA metabolism, oxidative DNA damage or chromatin winding. By contrast, if few or no factors interact, γH2AX signals will be respectively low or absent.

Besides, a mitotic-specific amplification of γH2AX preceding the apoptotic inter-nucleosomal DNA fragmentation has been detected in damaged cells starting mitosis [27]. Considering this finding, the overall chromosome γH2AX immunostaining observed in CHO9 metaphases (**Figure 1**) could correspond to an amplified pre-apoptotic $H2AX^{139}$ phosphorylation process.

Our results are in agreement with the assumption that mitotic γH2AX immunostaining is not a general phenomenon. In this sense, variability in the extent of $H2AX^{139}$ phosphorylation during mitosis among distinct cell lines (human HeLa and neuroblastoma, green monkey SV40 transformed kidney, C3H mouse embryo and *Indian muntjac* skin primary cultures) has been reported previously [21]. These observations indicate that H2AX phosphorylation is not a common feature of mitotic cells and that may be not indispensable for chromatin condensation during mitosis [33]. Further experimental approaches will elucidate the grounds of mitotic H2AX phosphorylation.

4.4. BLM-Induced γH2AX Signals Differed between Chromosomes and PMD Regions

γH2AX signals unrelated to BLM-exposure distributed uniformly among CHO9 chromosomes and PMD regions (t-test, $p > 0.001$; sign-test, $p > 0.0001$). This finding might indicate that basal γH2AX signals occur regularly per band unit. Conversely, BLM-induced γH2AX signals varied between chromosomes as follows: Z6 > Z2 > 2 > 5 > 1 > Z4 > Z1 > Z3 (sign-test, $p < 0.0001$) (**Figure 2**). Besides, BLM-induced γH2AX signals varied also between PMD regions. Chromosome segments close to centromeres showed low γH2AX signaling (sign-test, $p < 0.0001$) with a tendency to increase towards distal regions (**Figure 3**).

This uneven γH2AX signal distribution between chromosomes and chromosome regions is in agreement with the inter- and intra-chromosomal variability of the induced-damage reported by researchers of our laboratory in CHO cells [46]-[52] and others [53]-[61] both in human and in other mammalian cells.

4.5. Spontaneous and BLM-Induced γH2AX Signals Were Similar in CHO9 Homologous Chromosome Regions

Homologous regions are homologous chromosome segments among CHO9 chromosomes originated by rearrangements occurring during the cell line evolution. An equivalent γH2AX signal distribution in control and BLM-trated cells was detected between the partners of homologous regions (t-test, $p > 0.98$). Since chromatin features through homologous regions may be indistinguishable, the influence of the same chromatin structure in a particular chromosome region independently of the position in the karyotype could be put forward to explain this observation.

Chromosome regions of higher condensed chromatin (owing to compaction or protein coating) may be less accessible to chemical DNA damaging agents like BLM, and also less available to kinases related to $H2AX^{139}$ phosphorylation. Conversely, less condensed chromosome regions may be more sensitive to chemical agents and $H2AX^{139}$ phosphorylation kinases [47] [62] [63]. Since it is expected that along homologous regions similar chromatin states are present (*i e*. early replicating G-light bands, late replicating G-dark bands, heterochromatic constitutive C band, interstitial telomeric sequences) [64] [65], a comparable response to DNA damage and $H2AX^{139}$ phosphorylation is envisaged.

On the other hand, homologous regions from distinct chromosome pairs displayed differential sensitivity in $H2AX^{139}$ phosphorylation related to BLM. Interestingly, different γH2AX signal distributions were also observed between distinct homologous pairs belonging to the same chromosome, such as regions 1-Z1 and 1-Z6 of chromosome 1 (**Figure 4** and **Figure 6**). The distal 1-Z6 region revealed more $H2AX^{139}$ phosphorylation than 1-Z1. 1-Z6 homologous region is located distally on chromosome 1 and 1-Z1 expands through proximal, medial and distal segments of this chromosome. Therefore, the different sensitivity of chromatin states to damaging agents could explain the difference in γH2AX signaling between 1-Z1 and 1-Z6. In this respect, it was reported that regions with dissimilar chromatin organization may exhibit distinct sensibilities to chemical clastogens [47] [62].

Furthermore, the overall histone acetylation status of distinct interphase chromatin compartments is retained in metaphase chromosomes both in human and CHO9 metaphase chromosomes [66]. Less acetylated chromosome regions colocalize within G-dark and C-bands. On the contrary, hyperacetylated regions mainly correspond to G-light bands and gene-rich human telomeres (T-band regions) [66]-[68]. In this respect, the similarity between γH2AX signal and $H4^{+ac}$ profiles, increasing towards terminal CHO9 chromosome regions (**Figure 6(B)**) suggests that the organizational and functional state of the chromatin [37] [69] might underlie both types of epigenetic changes. However, more experimental evidences are required to support this hypothesis.

5. Conclusion

To sum up, γH2AX signals were detected in a high percentage of control metaphases, probably involving endogenous DNA damage or tensional stress. Nevertheless, it is clear that BLM exerted an effect on $H2AX^{139}$ phosphorylation, prevailing towards acetylated and gene-rich distal chromosome segments. Both basal and BLM-induced γH2AX signal distributions were equal between CHO9 homologous chromosome regions. The comparable $H2AX^{139}$ phosphorylation of homologous regions suggests its dependence on chromatin structure or function, being irrespective of the position in the karyotype. Co-immunostaining of γH2AX and proteins related to DDR, repair, apoptosis or chromatin remodeling as well as the induction of changes in chromatin status, could provide more information to understand the biological significance of basal mitotic $H2AX^{139}$ phosphorylation.

Acknowledgements

We thank PEDECIBA Postgraduate Program and the National Agency of Investigation and Innovation (ANNI) for financial support and G. Folle for critical reading of the manuscript.

References

[1] McKinnon, P.J. and Caldecott, K.W. (2007) DNA Strand Break Repair and Human Genetic Disease. *Annual Review of Genomics and Human Genetics*, **8**, 37-55. http://dx.doi.org/10.1146/annurev.genom.7.080505.115648

[2] Martin, O.A., Horikawa, I. and Zimonjic, D.B. (2004) Senescing Human Cells and Ageing Mice Accumulate DNA Lesions with Unrepairable Double-Strand Breaks. *Nature Cell Biology*, **6**, 168-170. http://dx.doi.org/10.1038/ncb1095

[3] Rouse, J. and Jackson, S.P. (2002) Interfaces between the Detection, Signaling and Repair of DNA Damage. *Science*, **297**, 547-551. http://dx.doi.org/10.1126/science.1074740

[4] Rogakou, E.P., Pilch, D.R., Orr, A.H., Ivanova, V.S. and Bonner, W.M. (1998) DNA Double-Stranded Breaks Induce Histone H2AX Phosphorylation on Serine 139. *Journal of Biological Chemistry*, **273**, 5858-5868. http://dx.doi.org/10.1074/jbc.273.10.5858

[5] Rogakou, E.P., Boon, C. and Redon, C. (1999) Megabase Chromatin Domains Involved in DNA Double-Strand Breaks *in Vivo*. *Journal of Cell Biology*, **146**, 905-916. http://dx.doi.org/10.1083/jcb.146.5.905

[6] Lou, Z., Minter-Dykhouse, K., Franco, S., Gostissa, M., Rivera, M.A., Celeste, A., Manis, J.P., van Deursen, J., Nussenzweig, A., Paull, T.T., Alt, W. and Chen, J. (2006) MDC1 Maintains Genomics Stability by Participating in the Amplification of ATM-Dependent DNA Damage Signals. *Molecular Cell*, **21**, 187-200.

http://dx.doi.org/10.1016/j.molcel.2005.11.025

[7] Bassing, C.H. and Alt, F.W. (2004) H2AX May Function as an Anchor to Hold Broken Chromosomal DNA Ends in Close Proximity. *Cell Cycle*, **3**, 149-153. http://dx.doi.org/10.4161/cc.3.2.684

[8] Huen, M.S., Grant, R. and Manke, I. (2007) RNF8 Transduces the DNA-Damage Signal via Histone Ubiquitylation and Checkpoint Protein Assembly. *Cell*, **131**, 901-914. http://dx.doi.org/10.1016/j.cell.2007.09.041

[9] Paull, T.T., Rogakou, E.P. and Yamazaki, V. (2000) A Critical Role for Histone H2AX in Recruitment of Repair Factors to Nuclear Foci after DNA Damage. *Current Biology*, **10**, 886-895. http://dx.doi.org/10.1016/S0960-9822(00)00610-2

[10] Svetlova, M., Solovjeva, L., Nishi, K., Nazarov, I., Siino, J. and Tomilin, N. (2007) Elimination of Radiation-Induced γH2AX Foci in Mammalian Nucleus Can Occur by Histone Exchange. *Biochemical and Biophysical Research Communications*, **358**, 650-654. http://dx.doi.org/10.1016/j.bbrc.2007.04.188

[11] Chowdhury, D., Xu, X. and Zhong, X. (2008) A PP4-Phosphatase Complex Dephosphorylates Gamma-H2AX Generated during DNA Replication. *Molecular Cell*, **31**, 33-46. http://dx.doi.org/10.1016/j.molcel.2008.05.016

[12] Macurek, L., Lindqvist, A., Voets, O., Kool, J., Vos, H.R. and Medema, R.H. (2010) Wip1 Phosphatase Is Associated with Chromatin and Dephosphorylates Gammah2ax to Promote Checkpoint Inhibition. *Oncogene*, **29**, 2281-2291. http://dx.doi.org/10.1038/onc.2009.501

[13] Bhogal, N., Kaspler, P. and Jalali, F. (2010) Late Residual Gamma-H2AX Foci in Murine Skin Are Dose Responsive and Predict Radiosensitivity *in Vivo*. *Radiation Research*, **173**, 1-9. http://dx.doi.org/10.1667/RR1851.1

[14] Banath, J.P., Klokov, D. and Macphail, S.H. (2010) Residual Gamma-H2AX Foci as an Indication of Lethal DNA Lesions. *BMC Cancer*, **10**, 4. http://dx.doi.org/10.1186/1471-2407-10-4

[15] Nelson, G., Buhmann, M. and von Zglinicki, T. (2009) DNA Damage Foci in Mitosis Are Devoid of 53BP1. *Cell Cycle*, **8**, 3379-3383. http://dx.doi.org/10.4161/cc.8.20.9857

[16] Nakamura, A.J., Rao, V.A., Pommier, Y., William, M. and Bonner, W.M. (2010) The Complexity of Phosphorylated H2AX Foci Formation and DNA Repair Assembly at DNA Double-Strand Breaks. *Cell Cycle*, **9**, 389-397. http://dx.doi.org/10.4161/cc.9.2.10475

[17] Sancar, A., Lindsey-Boltz, L.A., Ünsal-Kaçmaz, K. and Linn, S. (2004) Molecular Mechanisms of Mammalian DNA Repair and the DNA Damage Checkpoints. *Annual Review of Biochemistry*, **73**, 39-85. http://dx.doi.org/10.1146/annurev.biochem.73.011303.073723

[18] Rieder, C.L. and Cole, R.W. (1998) Entry into Mitosis in Vertebrate Somatic Cells Is Guarded by a Chromosome Damage Checkpoint That Reverses the Cell Cycle When Triggered during Early but Not Late Prophase. *The Journal of Cell Biology*, **142**, 1013-1022. http://dx.doi.org/10.1083/jcb.142.4.1013

[19] Chin, C.F. and Yeong, F.M. (2010) Safeguarding Entry into Mitosis: The Antephase Checkpoint. *Molecular and Cellular Biology*, **30**, 22-32. http://dx.doi.org/10.1128/MCB.00687-09

[20] Ichijima, Y., Sakasai, R., Okita, N., Asahina, K., Mizutani, S. and Teraoka, H. (2005) Phosphorylation of Histone H2AX at M Phase in Human Cells without DNA Damage Response. *Biochemical and Biophysical Research Communications*, **336**, 807-812. http://dx.doi.org/10.1016/j.bbrc.2005.08.164

[21] McManus, K.J. and Hendzel, M.J. (2005) ATM-Dependent DNA Damage-Independent Mitotic Phosphorylation of H2AX in Normally Growing Mammalian Cells. *Molecular Biology of the Cell*, **16**, 5013-5025. http://dx.doi.org/10.1091/mbc.E05-01-0065

[22] Giunta, S. and Jackson, S.P. (2011) Give Me a Break, but Not in Mitosis: The Mitotic DNA Damage Response Marks DNA Double-Strand Breaks with Early Signaling Events. *Cell Cycle*, **10**, 1215-1221. http://dx.doi.org/10.4161/cc.10.8.15334

[23] Giunta, S., Belotserkovskaya, R. and Jackson, S.P. (2010) DNA Damage Signaling in Response to Double-Strand Breaks during Mitosis. *The Journal of Cell Biology*, **190**, 197-207. http://dx.doi.org/10.1083/jcb.200911156

[24] Mukherjee, B., Kessinger, C., Kobayashi, J., Chen, B.P.C., Chen, D.J., Chatterjee, A., *et al.* (2006) DNA-PK Phosphorylates Histone H2AX during Apoptotic DNA Fragmentation in Mammalian Cells. *DNA Repair* (*Amst*), **5**, 575-590. http://dx.doi.org/10.1016/j.dnarep.2006.01.011

[25] Sluss, H.K. and Davis, R.J. (2006) H2AX Is a Target of the JNK Signaling Pathway That Is Required for Apoptotic DNA Fragmentation. *Molecular Cell*, **23**, 152-153. http://dx.doi.org/10.1016/j.molcel.2006.07.001

[26] Stucki, M. (2009) Histone H2AX Tyr142 Phosphorylation: A Novel Switch for Apoptosis? *DNA Repair* (*Amst*), **8**, 873-876. http://dx.doi.org/10.1016/j.dnarep.2009.04.003

[27] Varmark, H., Sparks, C.A., Nordberg, J.J., Koppetsch, B.S. and Theurkauf, W.E. (2009) DNA Damage-Induced Cell Death Is Enhanced by Progression through Mitosis. *Cell Cycle*, **8**, 2952-2964. http://dx.doi.org/10.4161/cc.8.18.9539

[28] Fulda, S. and Debatin, K.M. (2006) Extrinsic versus Intrinsic Apoptosis Pathways in Anticancer Chemotherapy. *On-*

cogene, **25**, 4798-4811. http://dx.doi.org/10.1038/sj.onc.1209608

[29] Solier, S. and Pommier, Y. (2009) The Apoptotic Ring: A Novel Entity with Phosphorylated Histones H2AX and H2B and Activated DNA Damage Response Kinases. *Cell Cycle*, **8**, 1853-1859. http://dx.doi.org/10.4161/cc.8.12.8865

[30] Modesti, M. and Kanaar, R. (2001) DNA Repair: Spot(light)s on Chromatin. *Current Biology*, **11**, R229-R232. http://dx.doi.org/10.1016/S0960-9822(01)00112-9

[31] Takai, H., Smogorzewskam, A. and de Lange, T. (2003) DNA Damage Foci at Dysfunctional Telomeres. *Current Biology*, **13**, 1549-1556. http://dx.doi.org/10.1016/S0960-9822(03)00542-6

[32] Pommier, Y., Barcelo, J.M., Rao, V.A., Sordet, O., Jobson, A.G., Thibaut, L., *et al*. (2006) Repair of Topoisomerase I-Mediated DNA Damage. *Progress in Nucleic Acid Research and Molecular Biology*, **81**, 179-229. http://dx.doi.org/10.1016/S0079-6603(06)81005-6

[33] Huang, X., Kurose, A., Tanaka, T., Traganos, F., Dai, W. and Darzynkiewicz, Z. (2006) Sequential Phosphorylation of *Ser*-10 on Histone H3 and *Ser*-139 on Histone H2AX and ATM Activation during Premature Chromosome Condensation: Relationship to Cell-Cycle Phase and Apoptosis. *Cytometry Part A*, **69A**, 222-229. http://dx.doi.org/10.1002/cyto.a.20257

[34] Puck, T.T., Cieciura S.J. and Robinson, A. (1958) Genetics of Somatic Mammalian Cells. III. Long-Term Cultivation of Euploid Cells from Human and Animal Subjects. *Journal of Experimental Biology*, **108**, 954-956.

[35] Deaven, L.L. and Petersen, D.F. (1973) The Chromosomes of CHO, an Aneuploid Chinese Hamster Cell Line: G-Band, C-Band, and Autoradiographic Analyses. *Chromosoma*, **41**, 129-144. http://dx.doi.org/10.1007/BF00319690

[36] Martínez-López, W., Boccardo, E., Folle, G.A., Porro, V. and Obe, G. (1998) Intrachromosomal Localization of Aberration Breakpoints Induced by Neutrons and G-Rays in Chinese Hamster Ovary Cells. *Radiation Research*, **150**, 585-592. http://dx.doi.org/10.2307/3579876

[37] Martínez-López, W., Folle, G.A., Obe, G. and Jeppesen, P. (2001) Chromosome Regions Enriched in Hyperacetylated Histone H_4 Are Preferred Sites for Endonuclease- and Radiation-Induced Breakpoints. *Chromosome Research*, **9**, 69-75. http://dx.doi.org/10.1023/A:1026747801728

[38] Wei, Y., Yu, L., Bowen, J., Gorovsky, M.A. and Allis, C.D. (1999) Phosphorylation of Histone H_3 Is Required for Proper Chromosome Condensation and Segregation. *Cell*, **97**, 99-109. http://dx.doi.org/10.1016/S0092-8674(00)80718-7

[39] Sauvé, D.M., Anderson, H.J., Ray, J.M., James, W.M. and Roberge, M. (1999) Phosphorylation-Induced Rearrangement of the Histone H_3 NH_2-Terminal Domain during Mitotic Chromatin Condensation. *The Journal of Cell Biology*, **145**, 225-235. http://dx.doi.org/10.1083/jcb.145.2.225

[40] Juan, G., Pan, W. and Darzynkiewicz, Z. (1996) DNA Segments Sensitive to Single Strand Specific Nucleases Are Present in Chromatin of Mitotic Cells. *Experimental Cell Research*, **227**, 197-202. http://dx.doi.org/10.1006/excr.1996.0267

[41] Pines, J. and Rieder, C.L. (2001) Re-Staging Mitosis: A Contemporary View of Mitotic Progression. *Nature Cell Biology*, **3**, 3-6.

[42] Mikhailov, A. and Rieder, C.L. (2002) Cell Cycle: Stressed Out of Mitosis. *Current Biology*, **12**, R331-R333. http://dx.doi.org/10.1016/S0960-9822(02)00833-3

[43] Tanaka, T., Halicka, H.D., Huang, X., Traganos, F. and Darzynkiewicz, Z. (2006) Constitutive Histone H2AX Phosphorylation and ATM Activation, the Reporters of DNA Damage by Endogenous Oxidants. *Cell Cycle*, **5**, 1940-1945. http://dx.doi.org/10.4161/cc.5.17.3191

[44] Skoufias, D.A., Lacroix, F.B., Andreassen, P.R., Wilson, L. and Margolis, R.L. (2004) Inhibition of DNA Decatenation, but Not DNA Damage, Arrests Cells at Metaphase. *Molecular Cell*, **15**, 977-990. http://dx.doi.org/10.1016/j.molcel.2004.08.018

[45] Castedo, M., Perfettini, J.L., Roumier, T., Andreau, K., Medema, R. and Kroemer, G. (2004) Cell Death by Mitotic catastrophe: A Molecular Definition. *Oncogene*, **23**, 2825-2837.

[46] Folle, G.A. and Obe, G. (1996) Intrachromosomal Localization of Breakpoints Induced by the Restriction Endonucleases Alu I and Bam HI in Chinese Hamster Ovary Cells Treated in S Phase of the Cell Cycle. *International Journal of Radiation Biology*, **69**, 447-457. http://dx.doi.org/10.1080/095530096145742

[47] Folle, G.A., Boccardo, E. and Obe, G. (1997) Localization of Chromosome Breakpoints Induced by DNase I in Chinese Hamster Ovary (CHO) Cells. *Chromosoma*, **106**, 391-399. http://dx.doi.org/10.1007/s004120050260

[48] Folle, G.A., Martínez-López, W., Boccardo, E. and Obe, G. (1998) Localization of Chromosome Breakpoints: Implication of the Chromatin Structure and Nuclear Architecture. *Mutation Research/Fundamental and Molecular Mechanisms of Mutagenesis*, **404**, 17-26. http://dx.doi.org/10.1016/S0027-5107(98)00090-6

[49] Martínez-López, W., Porro, V., Folle, G.A., Méndez-Acuña, L., Savage, J.R.K. and Obe, G. (2000) Interchromosomal

Distribution of Gamma Ray-Induced Chromatid Aberrations in Chinese Hamster Ovary (CHO) Cells. *Genetics and Molecular Biology*, **23**, 1071-1076. http://dx.doi.org/10.1590/S1415-47572000000400053

[50] Martínez-López, W., Folle, G.A., Cassina, G., Méndez-Acuña, L., Di-Tomaso, M.V., Obe, G. and Palitti, F. (2004) Distribution of Breakpoints Induced by Etoposide and X-Rays along the CHO X Chromosome. *Cytogenetic and Genome Research*, **104**, 182-187. http://dx.doi.org/10.1159/000077486

[51] Di Tomaso, M.V., Martínez-López, W., Folle, G.A. and Palitti, F. (2006) Modulation of Chromosome Damage Localization by DNA Replication Timing. *International Journal of Radiation Biology*, **82**, 877-886. http://dx.doi.org/10.1080/09553000600973335

[52] Di Tomaso, M.V., Martínez-López, W. and Palitti, F. (2010) Asynchronously Replicating Eu/Heterochromatic Regions Shape Chromosome Damage. *Cytogenetic and Genome Research*, **128**, 111-117. http://dx.doi.org/10.1159/000298820

[53] Barrios, L., Miró, R., Caballín, M.R., Fuster, C., Guedea, F., Subias, A. and Egozcue, J. (1989) Cytogenetic Effects of Radiotherapy Breakpoint Distribution in Induced Chromosome Aberrations. *Cancer Genetics and Cytogenetics*, **41**, 61-70. http://dx.doi.org/10.1016/0165-4608(89)90108-8

[54] Porfirio, B., Tedeschi, B., Vernole, P., Caporossi, D. and Nicoletti, B. (1989) The Distribution of *Msp* I-Induced Breaks in Human Lymphocyte Chromosomes and Its Relationship to Common Fragile Sites. *Mutation Research/Fundamental and Molecular Mechanisms of Mutagenesis*, **213**, 117-124. http://dx.doi.org/10.1016/0027-5107(89)90142-5

[55] Tedeschi, B., Porfirio, B., Caporossi, D., Vernole, P. and Nicoletti, B. (1991) Structural Chromosomal Rearrangements in *Hpa* II-Treated Human Lymphocytes. *Mutation Research/Fundamental and Molecular Mechanisms of Mutagenesis*, **248**, 115-121. http://dx.doi.org/10.1016/0027-5107(91)90093-4

[56] Slijepcevic, P. and Natarajan, A.T. (1994) Distribution of Radiation-Induced G1 Exchange and Terminal Deletion Break-Points in Chinese Hamster Chromosomes as Detected by G Banding. *International Journal of Radiation Biology*, **66**, 747-755.

[57] Slijepcevic, P. and Natarajan, A.T. (1994) Distribution of X-Rays-Induced G2 Chromatid Damage among Chinese Hamster Chromosomes: Influence of Chromatin Conformation. *Mutation Research Letters*, **323**, 113-119. http://dx.doi.org/10.1016/0165-7992(94)90084-1

[58] Xiao, Y. and Natarajan, A.T. (1999) Analysis of Bleomycin-Induced Chromosomal Aberrations in Chinese Hamster Primary Embryonic Cells by FISH Using Arm-Specific Painting Probes. *Mutagenesis*, **14**, 357-364. http://dx.doi.org/10.1093/mutage/14.4.357

[59] Obe, G., Johannes, C. and Schulte-Frohlinde, D. (1992) DNA Double-Strand Breaks Induced by Sparsely Ionizing Radiation and Endonucleases as Critical Lesions for Cell Death, Chromosomal Aberrations, Mutations and Oncogenic Transformation. *Mutagenesis*, **7**, 3-12. http://dx.doi.org/10.1093/mutage/7.1.3

[60] Schleiermacher, G., Janoueix-Lerosey, I., Combaret, V., Derré, J., Couturier, J., Aurias, A. and Delattre, O. (2003) Combined 24-Color Karyotyping and Comparative Genomic Hybridization Analysis Indicates Predominant Rearrangements of Early Replicating Chromosome Regions in Neuroblastoma. *Cancer Genetics and Cytogenetics*, **141**, 32-42. http://dx.doi.org/10.1016/S0165-4608(02)00644-1

[61] Janoueix-Lerosey, I., Hupe, P., Maciorowski, Z., La Rosa, P., Schleiermacher, G., Pierron, G., Liva, S., Barillot, E. and Delattre, O. (2005) Preferential Ocurrence of Chromosome Breakpoints within Early Replicating Regions in Neuroblastoma. *Cell Cycle*, **4**, 1842-1846. http://dx.doi.org/10.4161/cc.4.12.2257

[62] Folle, G.A. (2008) Nuclear Architecture, Chromosome Domains and Genetic Damage. *Mutation Research/Reviews in Mutation Research*, **658**, 172-183. http://dx.doi.org/10.1016/j.mrrev.2007.08.005

[63] Cowell, I.G., Sunter, N.J., Singh, P.B., Austin, C.A., Durkacz, B.W. and Tilby, M.J. (2007) γH2AX Foci Form Preferentially in Euchromatin after Ionising-Radiation. *PLoS ONE*, **2**, Article ID: e1057. http://dx.doi.org/10.1371/journal.pone.0001057

[64] Holmquist, G.P. (1992) Review Article: Chromosome Bands, Their Chromatin Flavor, and Their Functional Features. *American Journal of Human Genetics*, **51**, 17-37.

[65] Holmquist, G.P. and Ashley, T. (2006) Chromosome Organization and Chromatin Modification: Influence on Genome Function and Evolution. *Cytogenetic and Genome Research*, **114**, 96-125. http://dx.doi.org/10.1159/000093326

[66] Jeppesen, P. (1997) Histone Acetylation: A Possible Mechanism for the Inheritance of Cell Memory at Mitosis. *BioEssays*, **19**, 67-74. http://dx.doi.org/10.1002/bies.950190111

[67] Hebbes, T., Thorne, A.W. and Crane-Robinson, C. (1988) A Direct Link Between Core Histone Acetylation and Transcriptionally Active Chromatin. *The EMBO Journal*, **7**, 1395-1402.

[68] Turner, B.M. (2000) Histone Acetylation and an Epigenetic Code. *BioEssays*, **22**, 836-845. http://dx.doi.org/10.1002/1521-1878(200009)22:9<836::AID-BIES9>3.0.CO;2-X

[69] Martínez-López, W. and Di Tomaso, M.V. (2006) Chromatin Remodelling and Chromosome Damage. *Human & Experimental Toxicology*, **25**, 539-545. http://dx.doi.org/10.1191/0960327106het650oa